

A practical DMPs Implementation for Skill Creation and Teleoperation with Assistive Manipulators

Stefan Scherzinger¹, Pascal Becker¹, Arne Roennau¹ and Rüdiger Dillmann¹

Abstract—Assistive robotic manipulators are becoming increasingly important for people with disabilities. Teleoperating the manipulator in mundane tasks is part of their daily lives. Instead of steering the robot through all actions, applying self-recorded motion skills could greatly facilitate repetitive tasks. Dynamic Movement Primitives (DMP) are a powerful method for skill learning. For this use case, however, they need a simple heuristic to specify where to start and stop a skill without additional sensors. This paper provides the concept of *local*, *global*, and *hybrid* skills that form a modular basis for composing single-handed tasks with ease. A focus is on presenting the necessary mathematical details to support custom implementations with assistive robot arms. Experiments validate the developed methods for scratching an itchy spot, sorting objects on a desk, and feeding a piggy bank with coins. The paper is accompanied by an open-source implementation at <https://github.com/fzi-forschungszentrum-informatik/ArNe>

I. INTRODUCTION

Robotic manipulators are becoming increasingly important as assistive devices in home settings for people with disabilities. Despite the complexity of tasks of daily living - which often require two hands to accomplish - there are tasks that users can accomplish on their own with one robotic arm, such as organizing things on their desk, or scratching an itchy spot on the knee. Research shows promising hybrids between direct control and assistive autonomy for safe drinking [1], object manipulation [2],[3], and grasping [4], for instance. This autonomy, however, usually comes at the expense of additional sensor and hardware setups, e.g. [5], that must be provided and integrated into existing, basic manipulator systems. Losey et al show an approach for embedding high-dimensional robot behaviors into simplified, latent actions that users can then teleoperate [6]. Although improving users' performance in a kitchen setup, the behaviors must be demonstrated by caregivers first.

For the user group that can and wants to stay in cognitive control of their robot, a simple mechanism for recording repetitive motion patterns and replaying them might already be a big support. Steering the robot as a mere *tool* through teleoperation, users could flexibly create and personalize their own skill repertoire through programming by demonstration.

The principal contribution of the paper is a practical version of *Dynamic Movement Primitives* (DMPs) [7],[8],

This research has been funded by the Federal Ministry of Education and Research of Germany (BMBF) within the project ArNe in the framework of Robotic Systems in Health Care (project number 16SV8412)

¹ All authors are with FZI Research Center for Information Technology, Haid-und-Neu-Str. 10-14, 76131 Karlsruhe, Germany {scherzinger, becker, roennau, dillmann}@fzi.de

for recording and playing back such motion patterns while teleoperating robotic arms. Our concept targets six-axes manipulators without additional sensors for perception, and addresses the important challenge of formulating suitable start and goal states automatically for the DMPs during teleoperation. To this end, we propose *local*, *global*, and *hybrid* skills as a modular concept for composing everyday tasks. Our implementation simplifies much of the DMPs' complexity and additionally provides the necessary mathematical detail on coordinate transformations that are less often presented in papers. We accompany the paper with an implementation for the ROS framework [9], which is available open-source².

The remaining paper is structured as follows: We briefly describe the principle mechanisms behind DMPs in Section II to illustrate our simplifications to the original approach. Section III then describes our control interface for the manipulators. The core of the paper is Section IV with the presentation of three skill types and their implementation. We evaluate and discuss them in Section V, and provide an overall conclusion in Section VI.

II. BACKGROUND AND RELATED WORK

A. DMPs

The principle idea is to describe a trajectory $x(t)$ of a state vector $x \in \mathbb{R}^n$ of n dimensions with a set of ordinary differential equations (ODEs). In each dimension, its scalar variable x is defined by an individual spring-damper system, e.g.

$$\tau^2 \ddot{x} = K(g - x) - \tau D \dot{x} + (g - x_0) f(s) \quad . \quad (1)$$

Eq. (1) is usually referred to as *transformation system*. One important feature of DMPs is the generalization from new start states x_0 to new goals g , referred to as *attractor states*. The duration of the execution can be adjusted via the time scale τ . Both stiffness K and damping D are constants that need hand-tuning to specific use cases. Likewise, the arrangement of terms of Eq. (1) also varies with use cases and implementations. Popular enhancements include e.g. collision avoidance [10], [11] and the integration of haptic feedback [12]. Lauretti et al show a more recent approach for hybrid joint/Cartesian DMPs for redundant manipulators with the advantage of maintaining human-like motion during collision avoidance[13]. The non-linear *forcing term* $f(s(t))$ is the core of the framework, and is usually parameterized with a *phase variable* s across the course of the skill. This

²<https://github.com/fzi-forschungszentrum-informatik/ArNe>

term is responsible for effecting desired motion characteristics, which are to be learned from human-recorded training data.

All n transformation systems with the shape of Eq. (1) are synchronized through s according to the following *canonical system*

$$\tau \dot{s}(t) = -\alpha s(t) \quad (2)$$

that describes the correlation between phase time s and real-time t as an exponential decay from $1 \rightarrow 0$. The parameter α is an additional constant for fine-tuning.

The perturbation f is usually modeled with a superposition of radial basis functions, e.g.

$$f(s) = \frac{\sum_i \omega_i \psi_i(s)s}{\sum_i \psi_i(s)}, \quad (3)$$

with $\psi_i(s) = \exp(-h_i(s-c_i)^2)$ representing Gaussians with constant center c_i and constant width h_i . The higher the number of basis functions, and the more *clever* they overlap, the closer are they able to capture motion characteristics with f in Eq. (1). The choice of more suitable kernel functions can partially mitigate the exploding computational complexity and can allow for an a-priori estimation of the reproduction accuracy [14].

If combined with Reinforcement Learning (RL) on robots with many degrees of freedom, for instance, a massive number of basis functions can become a substantial performance bottleneck, since all parameters need to be learned and need to converge in numerous cycles of own trial and error[15].

Learning human skills supervised into DMPs means learning adjustable weights ω_i from example motions. This is achieved by recording a skill-defining trajectory $x(t), \dot{x}(t), \ddot{x}(t)$ of arbitrary duration from human demonstration. Solving Eq. (1) for f leads to a set of discrete samples by substituting the trajectory points into

$$\hat{f}(s(t)) = \frac{-K(g - x(t)) + \tau D\dot{x}(t) + \tau^2 \ddot{x}(t)}{g - x_0}. \quad (4)$$

This has a certain resemblance to an inverse dynamics approach, in which \hat{f} as reaction force is uniquely defined by the motion profile over time. The weights of Eq. (3) are then adjusted with the samples obtained from Eq. (4), e.g. by minimizing $\sum_s (\hat{f}(s) - f(s))^2$ with multivariate linear regression.

Finally, DMPs are deployed as follows: First Eq. (2) and then each of the n transformation systems with Eq. (1) are numerically integrated with a task-specific τ as a solution to an initial value problem. The combined state $x(t)$ is then passed to a suitable robot controller as a reference signal for motion tracking.

B. Assumptions and Simplifications

This paper describes a practical approach for using DMPs as a lightweight tool with a teleoperated manipulator. Composing and using skills on this basic system differs from what is often described in the literature. We assume that

- the users' creativity is unlimited in recording and playing-back skills

- the users must anticipate possible collisions themselves
- the playback of skills through the robot is open-loop
- the users will learn with this tool from trial and error.

It is worth pointing out that the core feature of generalization between different *attractor states* is achieved by the dynamical system itself, and solely depends on the shape of Eq. (1). For our case of modeling trajectories, the principle motivation for parameterizing f with overlapping basis functions is to provide a mechanism for time-independent scaling. There is usually a trade-off involved between capturing details in the motion profiles and being computationally tractable. An upper limit of accuracy would be an infinite number of basis functions. Considering our setting from above, the idea is as follows: If we use the same number of samples for describing recorded motion with Eq. (4) as for numerically integrating Eq. (1), then we can omit the complete parameterization. Temporal scaling would then be achieved with a mere assignment of timestamps to the computed motion. For instance, if we recorded a motion of 10 s at 100 Hz (= 1000 samples) and wanted to execute that in a different configuration during 20 s, we would numerically integrate Eq. (1) with a time step of 0.01 s (1000 steps), and a suitable controller would interpolate and follow these setpoints later at 50 Hz.

Our simplifications to the DMP approach summarize as follows:

- Set $\tau \equiv 1$ in Eq. (1)
- Drop Eq. (2), Eq. (3), and the phase variable s
- Use \hat{f} from Eq. (4) directly to integrate Eq. (1)

In the remainder of the paper, we apply these simplifications to our use case of teleoperating robotic manipulators with motion skills.

III. MANIPULATOR CONTROL

This section describes our methods for teleoperation and motion tracking. We target 6-axis light-weight robotic manipulators that are common as assistive devices. All grippers are suitable as long as their state can be mapped to a single degree of freedom. Fig. 1 illustrates one such manipulator with three important coordinate frames: the robot's base frame \mathcal{B} , the robot's end-effector frame \mathcal{E} , and its desired target pose \mathcal{X} during motion control. \mathcal{E} and \mathcal{X} are each defined by a position vector $\mathbf{x} = [x \ y \ z]^T \in \mathbb{R}^3$ and an orientation quaternion $\mathbf{q} = q_w + q_x i + q_y j + q_z k$, given in the base frame \mathcal{B} . The superscript d indicates *desired* quantities for target pose tracking. The end-effector frame \mathcal{E} is located at the grasping center of the 1-DOF gripper, whose state (opening percentage) is determined by the scalar $g \in [0, 1]$. The vector $\boldsymbol{\theta} \in \mathbb{R}^6$ denotes the set of joint angle positions. During motion control, a suitable controller continuously tracks the given target \mathcal{X} with the end-effector frame \mathcal{E} .

A. Teleoperation

Teleoperation must be simple and intuitive. Our approach uses a conventional space mouse as a 6-axis joystick, but similar low-cost devices could be used as well. This joystick measures infinitesimal displacements from interaction with

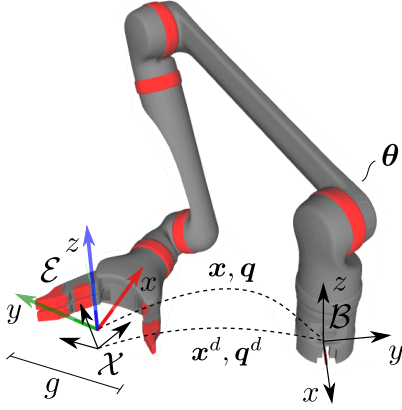


Fig. 1: Schematic illustration of our 6-axis light-weight robotic manipulator with base frame \mathcal{B} , end-effector frame \mathcal{E} , and desired target \mathcal{X} .

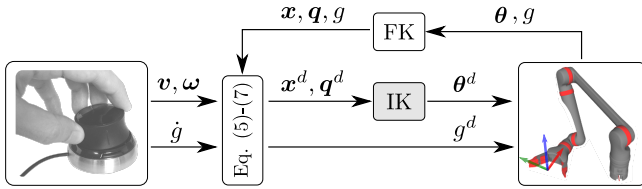


Fig. 2: Teleoperation with a 6-axis joystick. We integrate linear and angular velocity measurements into the desired target pose x^d, q^d for end-effector control. Additional buttons allow setting the opening and closing speed \dot{g} for the gripper.

thumb and fingers in three linear axes and three rotational axes, and interprets those signals as a combined, six-dimensional twist command $[v \ \omega]^T = [v_x \ v_y \ v_z \ \omega_x \ \omega_y \ \omega_z]^T$. Starting from the robot's end-effector frame \mathcal{E} in each control cycle, we then time-integrate this twist to become the new target pose \mathcal{X} for motion tracking according to

$$x^d = x + v\Delta t \quad (5)$$

$$q^d = q + \dot{q}\Delta t \quad , \quad \dot{q} = \frac{1}{2}\omega q \quad . \quad (6)$$

Fig. 2 shows the control scheme. All quantities are given in the robot's base frame \mathcal{B} . The quaternion product ωq uses the angular velocity given in quaternion notation $\omega = 0 + \omega_x i + \omega_y j + \omega_z k$. In a similar fashion, we time-integrate the gripper's opening/closing speed, which are triggered by pressing additional buttons on the joystick, to obtain its target state g^d with

$$g^d = g + \dot{g}\Delta t \quad . \quad (7)$$

The computation between Cartesian space and joint space is done with suitable *inverse kinematics* (IK) and *forward kinematics* (FK) algorithms.

B. Motion Tracking and Inverse Kinematics

The robots we target support streaming joint position control interfaces, i.e. they require θ^d at a specific control rate. We use a forward dynamics-based control approach

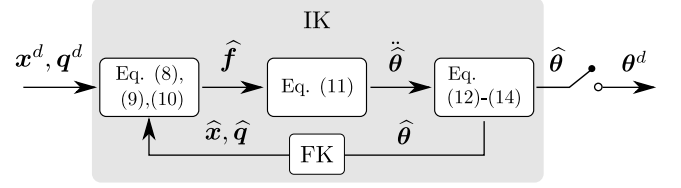


Fig. 3: Dynamics-based IK solver from our previous work [16], adapted to the notation of this paper. After internal iterations, the solver converges to a set of simulated joint positions $\hat{\theta}$ that best correspond to the given target pose.

of our previous work [16] for solving the IK problem during tracking the target pose \mathcal{X} . Its implementation is available open-source¹. In short, this IK solver transforms the difference between end-effector target \mathcal{X} and current pose \mathcal{E} into a 6-dimensional error. It then applies this error as a goal-directed force-torque vector at the end-effector of a virtual model of the robot, and closed-loop simulates the reaction motion of the system. The result θ^d is streamed to joint-level position controllers of the real system. Fig. 3 shows the control scheme, which we will briefly detail in the remainder of this section.

In the control scheme and succeeding equations, the hat symbol $\hat{(\cdot)}$ denotes *simulated* values. They are computed on a virtual model that equals the real robot's kinematics but has simplified dynamic properties.

The steps are as follows: First, we compute a virtual excitation \hat{f} from the translational and rotational error between the target and the current end-effector with

$$\hat{f} = K_p [\Delta x \ \Delta r]^T \quad . \quad (8)$$

The positive, diagonal stiffness matrix K_p serves as a proportional gain for this error. The individual error vectors are computed according to

$$\Delta x = x^d - \hat{x} \quad (9)$$

$$\Delta r = \phi [r_x \ r_y \ r_z]^T \leftarrow \Delta q = q^d \hat{q}^{-1} \quad , \quad (10)$$

in which Δq is the relative rotation between both frames in quaternion notation. We obtain the rotational error by transforming this rotation into *axis-angle* notation with the rotation angle ϕ and the normalized rotation axis $[r_x, r_y, r_z]^T$. The next step is to simulate the virtual system's response from this virtual excitation with

$$\ddot{\hat{\theta}} = \hat{H}^{-1} \hat{f} \quad . \quad (11)$$

\hat{H} is a dynamics-shaped joint space inertia matrix that leads to better linearization and convergence of the IK solver. We refer the interested reader to [17] for more details on this aspect. Since Eq. (11) delivers the motion response on acceleration level, the IK solver needs to integrate the joint accelerations $\ddot{\hat{\theta}}$ twice. We obtain $\hat{\theta}$ with the Euler forward

¹https://github.com/fzi-forschungszentrum-informatik/cartesian_controllers

method according to

$$\hat{\boldsymbol{\theta}}_t = \hat{\boldsymbol{\theta}}_{t-1} + \hat{\boldsymbol{\theta}}_{t-1} \Delta \hat{t} \quad (12)$$

$$\hat{\dot{\boldsymbol{\theta}}}_t = \hat{\dot{\boldsymbol{\theta}}}_{t-1} + \hat{\dot{\boldsymbol{\theta}}}_{t-1} \Delta \hat{t} . \quad (13)$$

Additional joint damping of 10% in each simulation cycle leads to an exponential decay of possible null space motion and avoids oscillations around the target pose:

$$\hat{\dot{\boldsymbol{\theta}}}_t \leftarrow 0.9 \hat{\dot{\boldsymbol{\theta}}}_t . \quad (14)$$

Note that the simulated step $\Delta \hat{t}$ is independent of the robot's real control rate Δt .

Finally, we use a common FK implementation from KDL² in the ROS framework to compute the simulated end-effector pose $\hat{\boldsymbol{x}}, \hat{\boldsymbol{q}}$ from the simulated joint positions in each cycle. The solver's result is the converged set of simulated joint positions $\hat{\boldsymbol{\theta}}$ that is then forwarded as the desired command for the streaming joint position interface of the robot.

IV. COMPOSING AND USING SKILLS

Motion skills are a central element for simplifying repetitive tasks. This section describes the methods behind building skills from recorded teleoperation, and details how we create new goal-oriented trajectories from these representations.

A. Skill Recording and Representation

We represent a specific robot state as the vector

$$\boldsymbol{s} = {}^{\mathcal{B}}[x, y, z, q_x, q_y, q_z, q_w, g] \quad (15)$$

that comprises the translation and orientation of \mathcal{E} , and the dimensionless gripper. All entities are given in the robot's base frame \mathcal{B} , and are computed from the joint positions $\boldsymbol{\theta}$ with forward kinematics. Using Cartesian coordinates for the state vector - as opposed to a joint-space representation - is important for motion generalization and shall make it easier to anticipate the robot's motion during skill playback for new targets. Equivalent to conventional DMPs, our skills capture motion characteristics from recorded state trajectories. We thus first teleoperate the robot and record a sequence of states $\{\boldsymbol{s}_0, \boldsymbol{s}_1, \boldsymbol{s}_2, \dots, \boldsymbol{s}_N\}$ in equidistant time steps Δt for a certain duration T . Fig. 4(a) illustrates an example of grasping an imaginary object and lifting it sideways in a slight arc.

We transform all recorded states with respect to the robot's end-effector frame when recording started. Since the skill will capture motion from this recording, it will do so in a neutral coordinate frame. We use homogeneous matrices for transformation, and denote $\boldsymbol{T}(\boldsymbol{s})$ for the homogeneous matrix representation of \boldsymbol{s} . Due to the quaternion notation of Eq. (15), formulating states as homogeneous matrices, and composing states back from the entries of a homogeneous matrix, is unique. With that, the states become

$$\boldsymbol{s}_n \leftarrow \boldsymbol{T}^{-1}(\boldsymbol{s}_0) \boldsymbol{T}(\boldsymbol{s}_n) , n = 0 \dots N . \quad (16)$$

Note that the gripper state g needs no transformation, and is simply kept throughout all coordinate systems. The first recorded state for any skill is thus $\boldsymbol{s}_0 = [0 \ 0 \ 0 \ 0 \ 0 \ 0 \ 1 \ g_0]^T$ with a gripper opening g_0 .

The next step is to compute the time derivatives $\dot{\boldsymbol{s}} = \frac{d}{dt}(\boldsymbol{s})$ and $\ddot{\boldsymbol{s}} = \frac{d}{dt}(\dot{\boldsymbol{s}})$, for which we use a five-step differentiator [18] with

$$\begin{aligned} \frac{d}{dt}(\boldsymbol{s}_n) := & \frac{5(\boldsymbol{s}_{n+1} - \boldsymbol{s}_{n-1})}{32\Delta t} + \frac{4(\boldsymbol{s}_{n+2} - \boldsymbol{s}_{n-2})}{32\Delta t} \\ & + \frac{\boldsymbol{s}_{n+3} - \boldsymbol{s}_{n-3}}{32\Delta t} \end{aligned} \quad (17)$$

that we apply to every state $n = 0 \dots N$ in the recorded sequence. Start and end boundaries are considered with

$$\boldsymbol{s}_{(\cdot)} = \begin{cases} \boldsymbol{s}_0 & \text{for } (\cdot) \leq 0 \\ \boldsymbol{s}_N & \text{for } (\cdot) \geq N \\ \boldsymbol{s}_{(\cdot)} & \text{else .} \end{cases} \quad (18)$$

We use Ijspeert's simple spring damper model [8] as transformation system, adapted to our state vector

$$\ddot{\boldsymbol{s}} = \boldsymbol{D}(\boldsymbol{K}(\boldsymbol{g} - \boldsymbol{s}) - \dot{\boldsymbol{s}}) + \boldsymbol{f} . \quad (19)$$

The vector \boldsymbol{g} stands for the goal state of the motion and will vary with skill *type* that we explain in the next section. The diagonal stiffness $\boldsymbol{K} \in \mathbb{R}^{8 \times 8}$ and damping matrix $\boldsymbol{D} \in \mathbb{R}^{8 \times 8}$ are chosen once, and remain constant throughout creating and using skills. Analog to the conventional DMP approach, we obtain n unique samples for the forcing term by solving Eq. (19) for \boldsymbol{f} and substituting the state trajectory in

$$\boldsymbol{f}_n = \ddot{\boldsymbol{s}}_n - \boldsymbol{D}(\boldsymbol{K}(\boldsymbol{g} - \boldsymbol{s}_n) - \dot{\boldsymbol{s}}_n) . \quad (20)$$

In contrast to conventional DMPs, however, the computed sequence of forcing terms $\{\boldsymbol{f}_0, \boldsymbol{f}_1, \boldsymbol{f}_2, \dots, \boldsymbol{f}_N\}$ already represents the quintessence of a skill.

B. Skill Types and Generalization

Skills are meant to be recorded at one point and replayed at another point. We propose three different *types* of skills that users can choose from to compose their everyday tasks: *local*, *global*, and *hybrid*. Each type will lead to a slightly different formulation of the goal state $\boldsymbol{g} \in \{\boldsymbol{g}_L, \boldsymbol{g}_G, \boldsymbol{g}_H\}$ in the transformation system Eq. (19), and will shape the path that the robot takes when applying the motion skill. The next sections present \boldsymbol{g} for each case.

1) *Local Skills*: This is the simplest type of generalization. The goal state is set to the final state as seen from the end-effector frame when we started the recording:

$$\boldsymbol{g}_L \leftarrow \boldsymbol{T}^{-1}(\boldsymbol{s}_0) \boldsymbol{T}(\boldsymbol{s}_N) . \quad (21)$$

It causes a simple playback of the recorded motion locally, starting from the robot's momentary end-effector frame \mathcal{E} . Fig. 4(b) shows the path that the robot would take for the example motion of Fig. 4(a).

²https://github.com/orocos/orocos_kinematics_dynamics

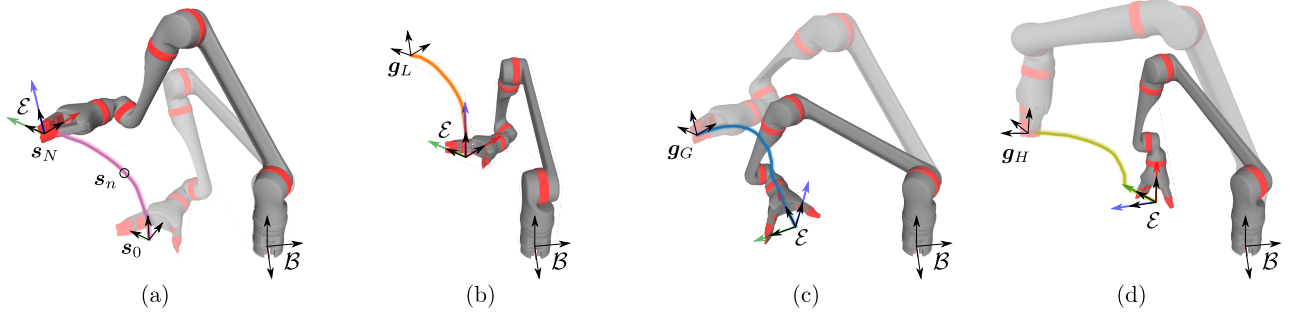


Fig. 4: Skill recording (a) and generalization with three different execution types: (b) *local* skill execution, (c) *global* execution, and (d) *hybrid* execution.

2) *Global Skills*: This type of skill sets the goal state to the final state of the recording and displays that in the current robot’s end-effector frame:

$$\mathbf{g}_G \leftarrow \mathbf{T}^{-1}(\mathbf{s}^*)\mathbf{T}(\mathbf{s}_N). \quad (22)$$

It causes a generalization back towards where the recorded motion ended, seen globally in the robot’s workspace. It starts from the robot’s momentary end-effector pose, denoted here with \mathbf{s}^* . Fig. 4(c) shows the effect, using the previous example motion.

3) *Hybrid Skills*: This type is a combination of local and global skills. It drives back to where the recorded motion globally ended but starts the motion with the momentary end-effector orientation. To achieve this, we make use of an additional frame that is adequately oriented in the robot’s end-effector frame and scale the local motion towards the global goal:

$$\mathbf{g}_H \leftarrow \mathbf{T}(\mathbf{g}_L) \begin{bmatrix} 0 \\ 0 \\ 0 \\ \frac{\|\mathbf{x}_G\|}{\|\mathbf{x}_L\|} \end{bmatrix}. \quad (23)$$

\mathbf{x}_G and \mathbf{x}_L denote the translational parts of \mathbf{g}_G and \mathbf{g}_L , respectively. Fig. 4(d) shows the respective path. We describe the details of the additional frame in the next section together with how all skills transform the created motion back to the robot’s base frame \mathcal{B} for control.

C. Trajectory Generation and Playback

Creating new trajectories is done in three steps. They all take place just before executing a skill in a new position. First, we compute a new sequence of states \mathbf{s}_n by numerically integrating Eq. (19) with one of the goal formulations from the previous section; then we transform this sequence back into the robot’s base frame for control; and finally assign desired timestamps for each state, and execute the motion with the robot.

1) *Numerical integration*: We integrate the transformation system with the forward Euler method. Algorithm 1 shows the scheme. Note that only the desired duration T of the skill and its type is chosen by the user. The other arguments are derived implicitly from the robot’s current pose in its workspace, such as the respective goal $\mathbf{g} \in \{\mathbf{g}_L, \mathbf{g}_G, \mathbf{g}_H\}$,

and the start for motion generation $\mathbf{s}_0, \dot{\mathbf{s}}_0$. Both \mathbf{f}_n and N are defined by the recorded skill.

Algorithm 1 Trajectory generation

```

1: procedure INTEGRATE( $\mathbf{g}, \mathbf{s}_0, \dot{\mathbf{s}}_0, \mathbf{f}_n, N, T$ )
2:    $\Delta t = T/N$ 
3:   for  $n = 1$  to  $N$  do
4:      $\mathbf{f}_{\parallel} = \frac{\mathbf{f} \cdot \mathbf{x}}{\|\mathbf{x}\|} \mathbf{x}$ 
5:      $\mathbf{f}_{\perp} = \mathbf{f} - \mathbf{f}_{\parallel}$ 
6:      $\mathbf{f}_{\parallel} = \frac{\|\mathbf{x}_G\|}{\|\mathbf{x}_L\|} \mathbf{f}_{\parallel}$ 
7:      $\mathbf{f} = \mathbf{f}_{\perp} + \mathbf{f}_{\parallel}$ 
8:      $\ddot{\mathbf{s}}_n = \mathbf{D}(\mathbf{K}(\mathbf{g} - \mathbf{s}_{n-1}) - \dot{\mathbf{s}}_{n-1})\mathbf{f}_n$ 
9:      $\dot{\mathbf{s}}_n = \dot{\mathbf{s}}_{n-1} + \ddot{\mathbf{s}}_n \Delta t$ 
10:     $\mathbf{s}_n = \mathbf{s}_{n-1} + \dot{\mathbf{s}}_n \Delta t$ 
11:   end for
12:   return  $\{\mathbf{s}_0, \mathbf{s}_1, \dots, \mathbf{s}_N\}$ 
13: end procedure

```

Step 4 to 7 rescale the translational part $\mathbf{f} \in \mathbb{R}^3$ of the forcing term $\mathbf{f}_n \in \mathbb{R}^8$ to take the new goal distance and the possibly changed stiffness into consideration. This is necessary, because the new goal attractor might pull harder than before, and might completely overrule the forcing term especially at the beginning of the generalization. We mitigate this effect by projecting \mathbf{f} onto the goal direction $\mathbf{x} \in \mathbb{R}^3$, scaling it, and re-adding the orthogonal component \mathbf{f}_{\perp} .

The result of Algorithm 1 is a sequence of N states that describe the new motion path in a skill-relative reference frame. Note that it is important to normalize the quaternion components afterward in the individual states before succeeding operations. Algorithm 1 works dimension-wise and does not enforce this.

2) *Transformations*: This step is to display the created sequence with respect to the robot’s base \mathcal{B} for the IK solver. Both *local* and *global* skills generalize the motion with respect to their momentary end-effector frame. Their motion is thus transformed with

$$\mathbf{s}_n \leftarrow \mathbf{T}(\mathbf{s}^*)\mathbf{T}(\mathbf{s}_n), n = 0 \dots N. \quad (24)$$

In contrast, *hybrid* skills generalize in a specialized reference frame, and need an additional rotation before transforming their states back to the robot base. Fig. 5 provides a

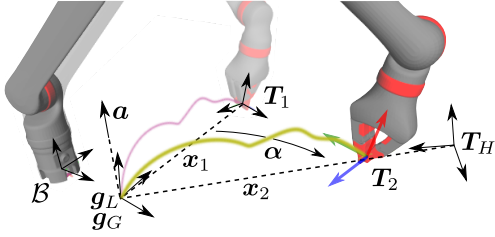


Fig. 5: Hybrid skill execution with recorded motion (purple) and projected motion (green) from a different start pose.

second example that we use to better illustrate the required steps. It shows a recorded motion that we apply from a different start pose. The two homogeneous transformation matrices

$$T_1 = T^{-1}(g_L) , \quad (25)$$

$$T_2 = T^{-1}(g_G) \quad (26)$$

represent the start of the example recording and the start of the *hybrid* generalization, respectively. Note that the recorded motion's local goal g_L and the global goal g_G always describe the same pose in the robot's workspace. Since *hybrid* skills shall drive to the global position while reproducing the motion from their local orientation, we need to rotate the recorded motion's start into the direction of T_2 with

$$T_H = T(\alpha, a)T_1 . \quad (27)$$

Fig. 5 shows the rotation angle α and the rotation axis a , which are defined by the two vectors x_1, x_2 , and whose components we directly obtain from T_1 and T_2 . Note that the length scaling of the motion is already considered with Eq. (23).

Finally, we extract the rotation $R \leftarrow T_2 T_H$ and display the motion in the end-effector's coordinates.

$$s_n \leftarrow \begin{bmatrix} R & \mathbf{0} \\ \mathbf{0}^T & 0 \end{bmatrix} T(s_n) , n = 0 \dots N . \quad (28)$$

After this operation, the states are given in frame \mathcal{E} and can be formulated in frame \mathcal{B} with Eq. (24).

3) *Trajectory duration and playback*: Users can specify the duration T of the skill that is fed into Algorithm 1. This is helpful if the motion is to be reproduced slower or faster than was recorded. Classic DMPs use a *canonical system* from Eq. (2) for this task and build the complete distribution of radial basis functions for approximating the forcing term f on this mechanism. Our practical approach circumvents this complexity by simply assigning the desired timestamp to each of the individual states of the sequence with

$$s^d(t) = \begin{cases} s_n \text{ with } n = \mathbb{N}(\frac{t}{\Delta t}) & \text{for } 0 \leq t < T \\ s_N & \text{for } T \leq t \end{cases} . \quad (29)$$

The notation $\mathbb{N}(\cdot)$ denotes a truncation and conversion into a natural number $n \in \mathbb{N}$. Each of the individual states s^d holds the desired robot control commands according to Eq. (15), and is passed to our IK solver as depicted in Fig. 6.

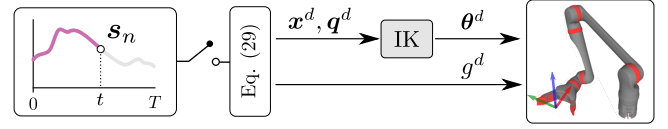


Fig. 6: Skill playback on the robotic manipulator with sampling desired gripper poses from the created state sequence. Our IK solver smoothly interpolates between these discrete targets for the robot's joint position control.

V. EXPERIMENTS AND RESULTS

This section demonstrates the feasibility of the proposed methods with applying *local*, *hybrid*, and *global* skills to example use cases. For each, we record a skill by teleoperating the robot through the motion once and apply the skill from various starting poses. We then plot and discuss the end-effector paths that the robot takes. The executions of all motions with the robot are shown in the accompanying video. In addition to this evaluation, we also give practical hints on how to mentally map everyday tasks to these three skill types.

A. Robotic Setup

We use the *Accrea Aria* robot for the experiments. It has an integrated gripper with one degree of freedom and three passive compliant fingers. Fig. 7(a) shows the arm in an upright position. It is compatible with ROS-control [19], and provides the necessary streaming interface for joint positions³. We use a *3DConnexion* spacemouse as joystick for teleoperating the robot. Stiffness and damping for Eq. (19) were set to $K = 0.55 \cdot I^{8 \times 8}$ and $D = 3.5 \cdot I^{8 \times 8}$, respectively.

B. Local Skill Evaluation

Local skills simply replay the recorded motion in the robot's current end-effector frame. This is useful for skills that can be formulated entirely central to some spot, such as wiping, brushing, or scratching. Fig. 7 shows a recorded brushing motion on a flat surface and various skill replays at slightly different spots. The curves show that the robot's end-effector replays the recorded pattern as expected.

C. Hybrid Skill Evaluation

This experiment evaluates our methods for goal-directed motions from different starting poses. Fig. 8(a) shows the setting. The robot is clamped to the table and the task is to collect softballs in a basket. If successful, all skill executions must terminate where the recording ended, independent from their start orientation, and the traveled path should reflect the characteristics of the recording. We conducted the experiment as follows: First, we teleoperated the robot once to record the skill. The recording started right before grasping the softball and ended after dropping it above the basket. We then teleoperated the robot manually to the remaining softballs and triggered the previously recorded skill at each spot with an open gripper. Fig. 8(b) shows the individual skill

³<https://github.com/stefanschertzinger/aria-ros/tree/devel>

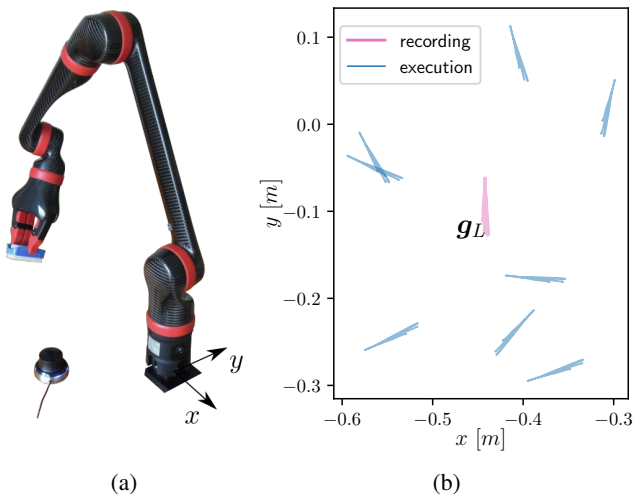


Fig. 7: (a): The robotic manipulator from our experiments with the joystick for teleoperation. (b) Brush movements on a flat surface, applied with a *local* skill at different positions and orientations.

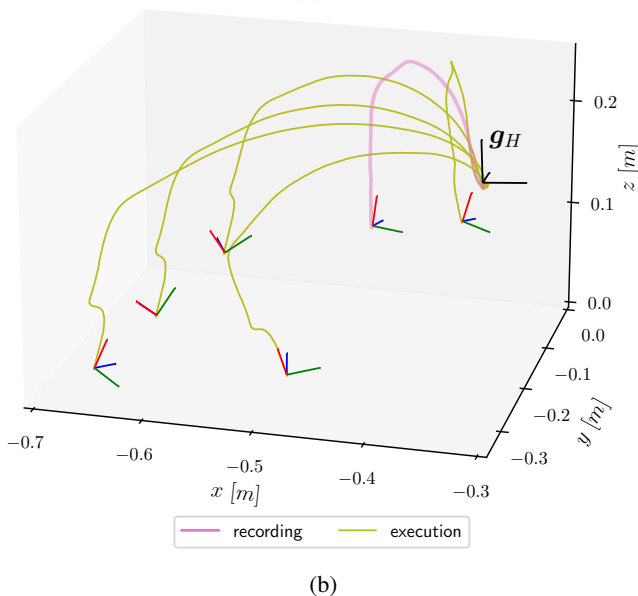
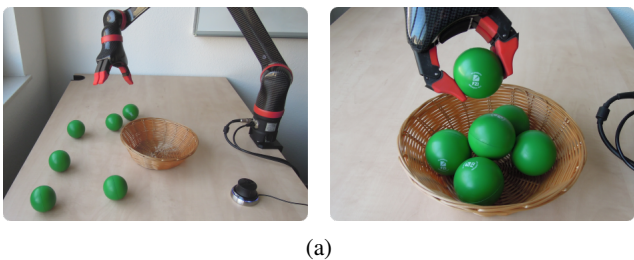


Fig. 8: (a) Collecting objects in a basket. (b) Recorded paths of the robot's end-effector with *hybrid* skill execution. A single recording is generalized from different starting poses.

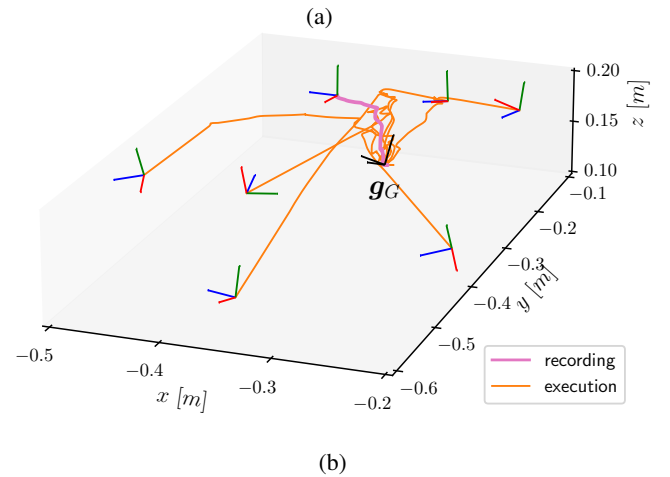


Fig. 9: (a) Feeding coins into a piggy bank from different starts. The coin's final orientation is essential for success. (b) Recorded paths of the *global* skill execution on the robot.

executions. The coordinate systems at the starts illustrate the gripper's orientation before grasping. All curves terminate in the hybrid goal g_H , as was intended, and the initial motion pattern is successfully scaled and reproduced with their orientation.

D. Global Skill Evaluation

This last experiment shows the generalization capabilities to exact goal poses. We feed a piggy bank as shown in Fig. 9(a), where the coin must be carefully aligned with the opening to succeed. While in the previous experiment the gripper mostly kept its local orientation during motion execution, this skill needs to generalize across the different quaternion dimensions to finally converge to the absolute goal pose. Fig. 9(b) shows the effectiveness of the presented methods. Note that the recorded motion was comparatively short and described a slight arc above the piggy. The skills, nevertheless, worked even from starts below this level and from significantly greater distances.

E. Discussion

Within our proposed framework, all goals are implicitly given through the last state of the motion recording. We think that this is a suitable trade-off between flexibility and ease of use, since it avoids that users need to specify Cartesian poses in the robot's workspace, and instead record what they want via teleoperation. Note that the presented methods do not aim for assistive autonomy, and there is no plausibility check whether the robot can execute a skill in the specified duration, nor whether a skill's motion might get distorted

through singular joint configurations. Instead, the approach is to give users cognitive responsibility and freedom over recording and deploying skills as they please, including to learn from trial and error.

Here are some examples to help map everyday tasks into our three categories:

- *Local skills*: Spooning food, opening doors and drawers, shaking a pack of juice, pouring, scratching an itchy spot
- *Hybrid skills*: Throwing things in a trash bin, putting ingredients in a pot, removing captured stones from a go board
- *Global skills*: Grasping and passing objects, bringing food to one’s mouth

Also, note that *hybrid* and *global* skills are mostly short-lived and make sense to be recorded immediately before executing a repetitive task. They could, however, be part of a permanent skill repertoire if the robot is mounted to a wheelchair, for instance, and the goals do not change with respect to the robot’s base.

VI. CONCLUSIONS

This paper presented a simplified DMPs-based approach for recording and playing-back skills with teleoperated manipulators. We proposed three skill types that can serve as a modular basis for simplifying repetitive patterns of everyday tasks. The skills take advantage of start and end states during recording and circumvent the difficulty of specifying goal attractors manually. By using the DMPs’ forcing term directly on the transformation system, we cut the complexity of parameterization with basis functions and the phase variable and instead realized time scaling with a simple reassigning of timestamps to fixed-step trajectories. These trajectories are then executed open-loop by an interpolating Cartesian controller. The presented methods target manipulator systems without sensors for perception and are suitable whenever users need a simple, tool-like mechanism to compose and use skills during teleoperation.

REFERENCES

- [1] Paolo Di Lillo et al. “BCI-Controlled Assistive Manipulator: Developed Architecture and Experimental Results”. In: *IEEE Transactions on Cognitive and Developmental Systems* 13.1 (2021), pp. 91–104.
- [2] Todor Stoyanov et al. “Assisted Telemanipulation: A Stack-Of-Tasks Approach to Remote Manipulator Control”. In: *2018 IEEE/RSJ International Conference on Intelligent Robots and Systems (IROS)*. 2018, pp. 1–9.
- [3] Ya-Ting Lee et al. “A self-reliance assistive tool for disable people”. In: *2018 3rd International Conference on Control and Robotics Engineering (ICCRE)*. 2018, pp. 26–30.
- [4] Siddarth Jain and Brenna Argall. “Grasp detection for assistive robotic manipulation”. In: *2016 IEEE International Conference on Robotics and Automation (ICRA)*. 2016, pp. 2015–2021.
- [5] Filippo Arrichiello et al. “Assistive robot operated via P300-based brain computer interface”. In: *2017 IEEE International Conference on Robotics and Automation (ICRA)*. 2017, pp. 6032–6037.
- [6] Dylan P. Losey et al. “Controlling Assistive Robots with Learned Latent Actions”. In: *2020 IEEE International Conference on Robotics and Automation (ICRA)*. 2020, pp. 378–384.
- [7] A. J. Ijspeert, J. Nakanishi, and S. Schaal. “Movement imitation with nonlinear dynamical systems in humanoid robots”. In: *Proceedings 2002 IEEE International Conference on Robotics and Automation (Cat. No.02CH37292)*. Vol. 2. 2002, 1398–1403 vol.2.
- [8] Auke Jan Ijspeert et al. “Dynamical movement primitives: learning attractor models for motor behaviors”. In: *Neural computation* 25.2 (2013), pp. 328–373.
- [9] Morgan Quigley et al. “ROS: an open-source Robot Operating System”. In: *ICRA workshop on open source software*. Vol. 3. 3.2. 2009, p. 5.
- [10] P. Pastor et al. “Learning and generalization of motor skills by learning from demonstration”. In: *2009 IEEE International Conference on Robotics and Automation*. 2009, pp. 763–768.
- [11] H. Hoffmann et al. “Biologically-inspired dynamical systems for movement generation: Automatic real-time goal adaptation and obstacle avoidance”. In: *2009 IEEE International Conference on Robotics and Automation*. 2009, pp. 2587–2592.
- [12] P. Pastor et al. “Towards Associative Skill Memories”. In: *2012 12th IEEE-RAS International Conference on Humanoid Robots (Humanoids 2012)*. 2012, pp. 309–315.
- [13] Clemente Lauretti, Francesca Cordella, and Loredana Zollo. “A hybrid joint/Cartesian DMP-based approach for obstacle avoidance of anthropomorphic assistive robots”. In: *International Journal of Social Robotics* 11.5 (2019), pp. 783–796.
- [14] Dimitrios Papageorgiou, Antonis Sidiropoulos, and Zoe Doulergi. “Sinc-Based Dynamic Movement Primitives for Encoding Point-to-point Kinematic Behaviors”. In: *2018 IEEE/RSJ International Conference on Intelligent Robots and Systems (IROS)*. 2018, pp. 8339–8345.
- [15] Adrià Colomé and Carme Torras. “Dimensionality Reduction for Dynamic Movement Primitives and Application to Bimanual Manipulation of Clothes”. In: *IEEE Transactions on Robotics* 34.3 (2018), pp. 602–615.
- [16] S. Scherzinger, A. Roennau, and R. Dillmann. “Inverse Kinematics with Forward Dynamics Solvers for Sampled Motion Tracking”. In: *19th International Conference on Advanced Robotics (ICAR)*. Dec. 2019, pp. 681–687.
- [17] Stefan Scherzinger, Arne Roennau, and Rüdiger Dillmann. *Virtual Forward Dynamics Models for Cartesian Robot Control*. 2020. arXiv: 2009.11888 [cs.RO].
- [18] Pavel Holoborodko. *Smooth Noise Robust Differentiators*. <http://www.holoborodko.com/pavel/numerical-methods/numerical-derivative/smooth-low-noise-differentiators/>. 2008.
- [19] Sachin Chitta et al. “ros_control: A generic and simple control framework for ROS”. In: *The Journal of Open Source Software* (2017).